

# SINCERE: Supervised Information Noise-Contrastive Estimation REvisited

Patrick Feeney and Michael C. Hughes

Dept. of Computer Science, Tufts University, Medford, MA, USA  
patrick.feeney@tufts.edu, michael.hughes@tufts.edu

February 20, 2024

## Abstract

The information noise-contrastive estimation (InfoNCE) loss function provides the basis of many self-supervised deep learning methods due to its strong empirical results and theoretic motivation. Previous work suggests a supervised contrastive (SupCon) loss to extend InfoNCE to learn from available class labels. However, in this work we find that the prior SupCon loss formulation has questionable justification because it can encourage some images from the same class to repel one another in the learned embedding space. We propose the Supervised InfoNCE REvisited (SINCERE) loss as a theoretically-justified supervised extension of InfoNCE that never causes images from the same class to repel one another. Experiments show that SINCERE leads to better separation of embeddings from different classes while delivering competitive classification accuracy for supervised and transfer learning. We further show an information-theoretic bound that relates SINCERE loss to the symmetrized KL divergence between data-generating distributions for a target class and all other classes.

## 1. Introduction

Self-supervised learning (SSL) has been crucial in creating pretrained computer vision models that can be efficiently adapted to a variety of tasks (Jing & Tian, 2020; Jaiswal et al., 2021). The conceptual basis for many successful pretraining methods is the instance discrimination task (Wu et al., 2018), where the model learns to classify each training image as a unique class. Self-supervised methods solve this task by *contrasting* different augmentations of the same image with other images, seeking a learned vector representation in which each image is close to augmentations of itself but far from others. Among several possible contrastive losses in the literature (Caron et al., 2020; Schroff et al.,

2015), one that has seen particularly wide adoption is information noise-contrastive estimation (InfoNCE) (van den Oord et al., 2018). InfoNCE variants such as MOCO (Chen et al., 2021), SimCLR (Chen et al., 2020a;b), and BYOL (Grill et al., 2020) have proven empirically effective.

The aforementioned methods are all for *unsupervised* pre-training of representations from unlabeled images. Instance discrimination methods may be extended for *supervised* applications to learn representations informed by the available class labels. A natural way forward is to contrast images of the same class with images from other classes (Schroff et al., 2015). The noise contrastive estimation framework (Gutmann & Hyvärinen, 2010) implements this idea by assuming that images from the same class are drawn from a target distribution while images from other classes come from a noise distribution.

Khosla et al. (2020) proposed the supervised contrastive (SupCon) loss as a supervised extension of the InfoNCE loss, forming target and noise distributions using supervised labels. Two straightforward ways of averaging the loss over pairs of images from the target distribution were examined. Their recommended loss, named SupCon, was chosen because it performed best empirically in top-1 classification on the ImageNet dataset (Deng et al., 2009). SupCon loss has been applied to problems such as contrastive open set recognition (Xu et al., 2023) and generalized category discovery (Vaze et al., 2022).

In light of this empirical success, we investigate the theoretical justification for SupCon in this work. We find that SupCon does not separate target and noise distributions well due to *inconsistent distribution definitions*. Consider a target class “dog” with at least 3 member images in the current batch, referred to as  $S$ ,  $p$ , and  $a$  as illustrated in Fig. 1. To compute the SupCon objective, we select a target image  $S$  and a same-class partner  $p$  (ultimately averaging over such

Open-source Code: <https://github.com/tufts-ml/SupContrast>

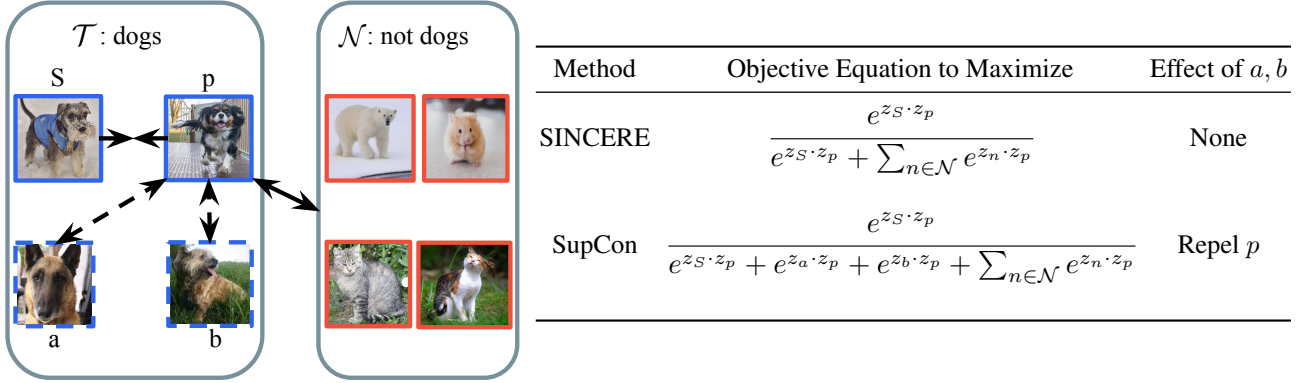


Figure 1. Visualization of supervised contrastive learning objectives for pulling together embeddings from the target class, indexed by elements of  $\mathcal{T}$ , and pushing away embeddings from the noise classes, indexed by elements of  $\mathcal{N}$ . Both objectives are defined with respect to a pair of target embeddings  $z_S$  and  $z_p$ . Solid arrows show *common* effects of both methods:  $z_p$  is pulled towards  $z_S$  and pushed away from embeddings  $z_n$  from the noise classes. Dashed arrows show a *problematic effect of SupCon*:  $z_p$  is pushed away from  $z_a$  and  $z_b$  as if they were from a noise class, despite belonging to the target class.

pairs). Optimizing SupCon pulls embeddings of  $S$  and  $p$  together, but problematically treats dog image  $a$  as a noise image and pushes  $p$ 's representation away from  $a$ . This inconsistency makes it difficult to separate target and noise classes in the embedding space. Moreover, the problem will get worse as the number of target-class images increases and more target images are treated as noise.

To resolve this issue, this paper proposes the Supervised InfoNCE REvisited (SINCERE) loss. Unlike SupCon, SINCERE loss excludes target images such as  $a$  in Fig. 1 from the noise distribution, thus ensuring *consistent* target and noise distributions as in InfoNCE.

Overall, our main contributions are:

1. A demonstration of the problematic effects of SupCon loss' within-class repulsion through a formal analysis of gradients and an empirical investigation of the separation of classes in the learned embeddings.
2. The SINCERE loss function, which is a drop-in replacement for SupCon loss for supervised representation learning. We derive the SINCERE loss from a probabilistic model while enforcing a core assumption of noise-contrastive estimation: images known to be from target distribution should not be treated as noise examples. SINCERE is thus a well-founded generalization of InfoNCE that can use available class labels.
3. A proof that our idealized SINCERE loss acts as an upper bound on the negative symmetrized KL divergence between the data-generating target and noise distributions. This information-theoretic analysis sheds light on how the number of noise samples and the similarity of target and noise distributions impact loss values.

4. Empirical results showing that SINCERE loss eliminates the problematic within-class repulsion behavior of the SupCon loss while delivering competitive accuracy for supervised learning and superior accuracy for transfer learning.

Ultimately, practitioners that use SINCERE can enjoy the same or better downstream classification accuracy as SupCon while benefiting from a solid conceptual foundation and *improved separation* of target and noise distributions in learned embedding space. Code for reproducing all experiments is available via the code supplement.

## 2. Background

### 2.1. Noise-Contrastive Estimation

Noise-contrastive estimation (NCE) (Gutmann & Hyvärinen, 2010) provides a general framework for modeling a target distribution of interest given a set of samples from it. This framework utilizes a binary classifier to contrast the target distribution samples with samples from a noise distribution. This noise distribution is an arbitrary distribution different from the target distribution, although in practice the noise distribution must be similar enough to the target distribution to make the classifier learn the structure of the target distribution. Works described in subsequent sections maintain the focus on contrasting target and noise distributions while defining these distributions as generating disjoint subsets of a dataset of interest.

### 2.2. Self-Supervised Contrastive Learning

To begin, we introduce notation used throughout this paper. See also the notation summary in Table A.1 for easy refer-

ence. Consider an observed dataset  $(\mathcal{X}, \mathcal{Y})$  of  $N$  elements. Let  $\mathcal{X} = (x_1, x_2, \dots, x_N)$  define the data features (e.g. images), and  $\mathcal{Y} = (y_1, y_2, \dots, y_N)$  the categorical labels. Each example (indexed by integer  $i$ ) has a feature vector  $x_i$  paired with an integer-valued categorical label  $y_i \in \llbracket 1, K \rrbracket$ , where  $K$  indicates the number of classes and  $2 \leq K \leq N$ . Let integer interval  $\mathcal{I} = \llbracket 1, N \rrbracket$  denote the set of possible indices for elements in  $\mathcal{X}$  or  $\mathcal{Y}$ .

Self-supervised contrastive learning pursues an *instance discrimination* task (Wu et al., 2018) to learn effective representations. This involves treating each example in the dataset as a separate class. Therefore each example  $i$  has a *unique* label  $y_i$  and the number of classes  $K$  is equal to  $N$ .

To set up the instance discrimination problem, let  $S \in \mathcal{I}$  denote the index of the only member of the target distribution in the dataset. Let the rest of the dataset  $\mathcal{N} = \mathcal{I} \setminus \{S\}$  be drawn from the noise distribution. Applying NCE produces the Information Noise-Contrastive Estimation (InfoNCE) loss (van den Oord et al., 2018)

$$L_{\text{InfoNCE}}(x_S, y_S) = -\log \frac{e^{f(x_S, y_S)}}{e^{f(x_S, y_S)} + \sum_{n \in \mathcal{N}} e^{f(x_n, y_S)}} \quad (1)$$

where  $f(x_i, y_j)$  is a classification score function which outputs a scalar score for image  $x_i$  where greater values indicate that label  $y_j$  is more likely. When  $y_S$  denotes the target class, loss  $L_{\text{InfoNCE}}(x_S, y_S)$  thus calculates the negative log-likelihood that index  $S$  correctly locates the only sample from the target class.

The function  $f$  is often chosen to be cosine similarity by representing both terms as vectors in an embedding space (Wu et al., 2018; Chen et al., 2020a; 2021). Let  $z_i \in \mathbb{R}^D$  be a  $D$ -dimensional unit vector representation of data element  $x_i$  produced by a neural network. Embeddings are also used to represent  $y_S$ , so let  $z'_S$  be a second representation of  $x_S$ .  $z'_S$  can be produced by embedding a data augmented copy of  $x_S$  (Le-Khac et al., 2020; Chen et al., 2020a), embedding  $x_S$  via older (Wu et al., 2018) or averaged (Chen et al., 2021) embedding function parameters, or a combination of these techniques (Jaiswal et al., 2021).

Rewriting  $L_{\text{InfoNCE}}$  in terms of a data augmented  $z'_S$  and setting  $f(z_i, z_j) = z_i \cdot z_j / \tau$ , with  $\tau$  acting as a temperature hyperparameter, produces the self-supervised contrastive loss proposed by Wu et al. (2018):

$$L_{\text{self}}(z_S, z'_S) = -\log \frac{e^{z_S \cdot z'_S / \tau}}{e^{z_S \cdot z'_S / \tau} + \sum_{n \in \mathcal{N}} e^{z_n \cdot z'_S / \tau}} \quad (2)$$

Note that each embedding vector is a unit vector so the dot products will always be in  $[-1, 1]$  before scaling by  $\tau$ .

InfoNCE and the subsequent self-supervised contrastive losses cited previously are all theoretically motivated by NCE. The larger instance discrimination problem is posed as a series of binary classification problems between instance-

specific target and noise distributions. This clear distinction between target and noise underlies our later SINCERE loss.

### 2.3. Supervised Contrastive Learning (SupCon)

In the supervised setting, labels  $y_i$  are no longer unique for each data point. Instead, we assume a fixed set of  $K$  known classes, such as “dogs” and “cats,” with multiple examples in each class. Again, the larger  $K$ -way discrimination task is posed as a series of binary NCE tasks. Each binary task distinguishes one target class from a noise distribution made up of the  $K - 1$  remaining classes.

Let index  $S$  again denote a selected instance that defines the current target class  $y_S$ . Let  $\mathcal{T} = \{i \in \mathcal{I} | y_i = y_S\}$  be the set of all elements from the target class: unlike the self-supervised case, here  $\mathcal{T}$  has *multiple* elements. Let the possible set of same-class partners for index  $S$  be  $\mathcal{P} = \mathcal{T} \setminus \{S\}$ . Let the set of indices from the noise distribution be  $\mathcal{N} = \mathcal{I} \setminus \mathcal{T}$ .

Khosla et al. (2020) propose a supervised contrastive loss known as “SupCon”. For chosen  $S$ , the loss is  $\frac{-1}{|\mathcal{P}|} \sum_{p \in \mathcal{P}} L_{\text{SupCon}}(z_S, z_p)$ , with  $L_{\text{SupCon}}(z_S, z_p)$  defined as

$$-\log \frac{e^{z_S \cdot z_p / \tau}}{(\sum_{j \in \mathcal{T} \setminus \{p\}} e^{z_j \cdot z_p / \tau}) + \sum_{n \in \mathcal{N}} e^{z_n \cdot z_p / \tau}}. \quad (3)$$

Here,  $p \in \mathcal{P}$  denotes another index from the target class.

Khosla et al. (2020) suggest this loss as a “straightforward” extension of  $L_{\text{self}}$  to the supervised case, with the primary justification given via their reported empirical success on ImageNet (Deng et al., 2009) classification.

We notice that this loss contains terms from the target distribution in the denominator (those indexed by  $j$  when  $j \neq S$ ) that are not in the numerator when  $|\mathcal{P}| > 1$ . In contrast, the self-supervised loss in Eq. (2) includes all target terms in both numerator and denominator. SupCon’s choice to have some target examples only in the denominator of Eq. (3) effectively treats them as part of the noise distribution. That is, the SupCon loss will learn to push such embeddings  $z_j$  away from  $z_p$ , as in Fig. 1. This problematic behavior complicates analysis of the loss (Graf et al., 2021) and limits SupCon’s ability to separate embeddings by class.

## 3. Method

In this section, we develop a new loss for supervised contrastive learning called SINCERE. We derive and justify our SINCERE loss in Sec. 3.1, showing how it arises from applying noise-contrastive estimation to a supervised problem via the same probabilistic principles that justify InfoNCE for the self-supervised case. In fact, the self-supervised case becomes a special case of our proposed SINCERE framework. Sec. 3.2 describes a practical implementation

of SINCERE. Sec. 3.3 contrasts the gradient of SINCERE with the gradient of SupCon loss. Sec. 3.4 motivates the loss via an information-theoretic bound. Finally, Sec. 3.5 examines how SINCERE loss relates to other works building on InfoNCE and SupCon losses.

### 3.1. Derivation and Justification

We first review the principles that establish InfoNCE loss as suitable for the self-supervised learning case. We then extend that derivation to the more general supervised case. In each case, we establish a data-generating probabilistic model involving a target and a noise distribution. This model gives rise to a one-from-many selection task. Our proposed SINCERE loss, like InfoNCE before it, is then interpreted as a negative log likelihood of a tractable neural network approximation to this model.

#### 3.1.1. SELF-SUPERVISED CASE

In the self-supervised case, instance discrimination is posed as a series of binary target-noise discrimination tasks. Each target distribution produces images that depict a specific instance (e.g. data augmentations of a single image). The corresponding noise distribution generates images of other possible instances. Throughout this subsection, we focus analysis on *just one* of these binary tasks, treating its target distribution and noise distribution as fixed. Sec. 3.2 will describe how our approach models multiple target-noise tasks.

**Assumption 3.1.** We observe a dataset  $\mathcal{X}$  of  $N$  examples with unknown labels such that exactly one example’s data is drawn from the target distribution.

Let random variable  $S \in \mathcal{I}$  indicate the index of the example sampled from the target distribution with PDF  $p^+(x_i)$ . All other examples  $\mathcal{N} = \mathcal{I} \setminus \{S\}$  are drawn i.i.d. from the noise distribution with PDF  $p^-(x_i)$ .

**Definition 3.2.** The “true” data-generating model for the self-supervised case, under the above assumptions, is

$$p(S) = \text{Unif}(\mathcal{I}) \quad (4)$$

$$p(\mathcal{X}|S) = p^+(x_S) \prod_{n \in \mathcal{N}} p^-(x_n) \quad (5)$$

$$p(\mathcal{X}, S) = p(\mathcal{X}|S)p(S) \quad (6)$$

where  $\text{Unif}(\mathcal{I})$  is the uniform distribution over indices.

This model is used to solve a selection task: given dataset  $\mathcal{X}$ , which index is from the target class?

**Proposition 3.3.** Assume  $\mathcal{X}$  is generated from (6) and that the target and noise PDFs are known. The probability that

index  $S$  is the sole draw from the target distribution is

$$p(S|\mathcal{X}) = \frac{p^+(x_S) \prod_{n \in \mathcal{N}} p^-(x_n)}{\sum_{i \in \mathcal{I}} p^+(x_i) \prod_{j \in \mathcal{I} \setminus \{i\}} p^-(x_j)} \quad (7)$$

$$= \frac{\frac{p^+(x_S)}{p^-(x_S)}}{\frac{p^+(x_S)}{p^-(x_S)} + \sum_{n \in \mathcal{N}} \frac{p^+(x_n)}{p^-(x_n)}}. \quad (8)$$

*Proof.* Bayes theorem produces the first formula given the joint  $p(S, \mathcal{X})$  defined in (6). Algebraic simplifications lead to the second formula, recalling  $\mathcal{I} = \mathcal{N} \cup \{S\}$ .  $\square$

The above formalizes a result from van den Oord et al. (2018) used to motivate their InfoNCE loss. As will be shown more formally in Section 3.1.3, a neural network  $f$  that learns to approximate the ratio  $\frac{p^+(x_i)}{p^-(x_i)}$  minimizes InfoNCE loss.

#### 3.1.2. SUPERVISED CASE

In the supervised case, supervised classification is posed as a series of binary target-noise discrimination tasks. Each target distribution produces images that depict a single class, such as “dog.” The corresponding noise distribution generates images of all other classes, such as “cat” and “hamster.”

**Assumption 3.4.** We observe a dataset  $\mathcal{X}$  of  $N$  examples with unknown labels such that exactly  $2 \leq T < N$  examples’ data is drawn from the target distribution.

Let random variable  $\mathcal{P} \in \{I \subset \mathcal{I} \mid |I| = T - 1\}$  indicate  $T - 1$  indices identifying all but one of the examples from the target distribution. Let random variable  $S \in \mathcal{I} \setminus \mathcal{P}$  indicate the index of the final example sampled from the target distribution. The set of all indices from the target distribution is denoted  $\mathcal{T} = \mathcal{P} \cup \{S\}$ . The remaining indices  $\mathcal{N} = \mathcal{I} \setminus \mathcal{T}$  are drawn i.i.d. from the noise distribution.

**Definition 3.5.** The “true” data-generating model for the supervised case is

$$p(\mathcal{P}) = \text{Unif}(\{I \subset \mathcal{I} \mid |I| = T - 1\}) \quad (9)$$

$$p(S|\mathcal{P}) = \text{Unif}(\mathcal{I} \setminus \mathcal{P}) \quad (10)$$

$$p(\mathcal{X}|\mathcal{P}, S) = p^+(x_S) \prod_{p \in \mathcal{P}} p^+(x_p) \prod_{n \in \mathcal{N}} p^-(x_n) \quad (11)$$

$$p(\mathcal{X}, \mathcal{P}, S) = p(\mathcal{X}|\mathcal{P}, S)p(S|\mathcal{P})p(\mathcal{P}) \quad (12)$$

where  $\mathcal{P}$ ’s distribution is the uniform distribution over sets of exactly  $T - 1$  distinct indices within the larger set  $\mathcal{I}$ .

In the special case of  $T = 1$ , note that  $\mathcal{P}$  becomes the empty set, and the supervised model in (12) (where knowledge of  $\mathcal{P}$  provides additional information about the target class) reduces to the simpler self-supervised model in (6).

The following likelihood generalizes (8) for the supervised case and motivates the SINCERE loss.



**Proposition 3.6.** Assume  $\mathcal{X}$  and  $\mathcal{P}$  are generated from (12) and that the target and noise PDFs are known. The probability that any index  $S$  in  $\mathcal{I} \setminus \mathcal{P}$  is the final draw from the target distribution is

$$p(S|\mathcal{X}, \mathcal{P}) = \frac{\frac{p^+(x_S)}{p^-(x_S)}}{\frac{p^+(x_S)}{p^-(x_S)} + \sum_{n \in \mathcal{N}} \frac{p^+(x_n)}{p^-(x_n)}}. \quad (13)$$

*Proof.* We first derive an expression for  $p(S, \mathcal{P}|\mathcal{X})$  from the joint defined in (12). Standard probability operations (sum rule, product rule) then allow obtaining the desired  $p(S|\mathcal{P}, \mathcal{X})$ . For details, see App. B.  $\square$

In contrast to SINCERE, attempts to translate SupCon loss into the noise-contrastive paradigm do *not* result in a coherent probabilistic model, as detailed in App. D. In short, SupCon does not form a valid PMF  $p(S|\mathcal{X}, \mathcal{P})$  due to the extra target class terms in its loss’ denominator.

### 3.1.3. TRACTABLE MODEL

In practice, we will not know the true density functions for target or noise distributions, as assumed in (13). Instead, given only  $\mathcal{X}$  and  $\mathcal{P}$  we can build an alternative tractable model for determining the index  $S$  of the final member of the target class.

**Definition 3.7.** Let neural net  $f_\theta(x_i, y_S)$ , with parameters  $\theta$ , map any input data  $x_i$  and target class  $y_S$  to a real value indicating the relative confidence that  $x_i$  belongs to the target class (greater value is more confident). Our tractable model for  $S$  given data  $\mathcal{X}$  and known class members  $\mathcal{P}$  is

$$p_\theta(S|\mathcal{X}, \mathcal{P}) = \frac{e^{f_\theta(x_S, y_S)}}{e^{f_\theta(x_S, y_S)} + \sum_{n \in \mathcal{N}} e^{f_\theta(x_n, y_S)}}. \quad (14)$$

Suppose we can observe many samples of  $\mathcal{X}, \mathcal{P}, S$  from the true model in (12). We can fit  $f_\theta$  by minimizing the following *idealized* SINCERE loss

$$L_{\text{SINCERE}}(\theta) = \mathbb{E}_{\mathcal{X}, S, \mathcal{P}} [-\log p_\theta(S|\mathcal{P}, \mathcal{X})] \quad (15)$$

where the expectation is over samples from the generative model (12).

Our proposed SINCERE loss provides a principled way to fit a tractable neural model  $f_\theta$  to identify the last remaining member of a target class when given other class member indices  $\mathcal{P}$ . We justify the chosen form of function in (14) and loss  $L_{\text{SINCERE}}$  in (15) in two steps. First, we suggest it is possible to set parameters  $\theta$  to a value  $\theta^*$  such that the tractable model  $p_{\theta^*}(S|\mathcal{X}, \mathcal{P})$  exactly matches the true distribution  $p(S|\mathcal{X}, \mathcal{P})$ . Second, we prove this matching parameter  $\theta^*$  will be a minimizer of the SINCERE loss. This justification for the loss holds for both the supervised case that is our main focus, as well for the self-supervised case where  $\mathcal{P}$  is the empty set. The assumption and theorem below can be viewed as a formalization of the arguments

in van den Oord et al. (2018) that have been extended to handle the supervised case in a principled way.

**Assumption 3.8.** The function class of neural network  $f_\theta$  is sufficiently flexible, such that there exists parameters  $\theta^*$  satisfying  $e^{f_{\theta^*}(x_i, y_S)} = \frac{p^+(x_i)}{p^-(x_i)}$  for all data vectors  $x_i$ .

Universal approximation theorems for neural networks (Lu et al., 2017) suggest this function approximation task is achievable.

**Theorem 3.9.** Parameters  $\theta^*$  minimize the SINCERE loss defined in (15), where the expectation is over samples of  $\mathcal{X}, S, \mathcal{P}$  from the generative model (12).

*Proof.* The loss minimization objective (15) is equivalent to maximizing the tractable log likelihood  $p_\theta(S|\mathcal{X}, \mathcal{P})$  under samples from the generative model. The theory of maximum likelihood estimation under possible model misspecification (White, 1982; Fan, 2016) shows this is equivalent to minimizing the KL-divergence  $D_{\text{KL}}(p_{\text{true}}(S|\mathcal{X}, \mathcal{P}) || p_\theta(S|\mathcal{X}, \mathcal{P}))$ , where  $p_{\text{true}}(S|\mathcal{X}, \mathcal{P})$  is the likelihood from the generative model. KL-divergence is minimized and equal to 0 when its two arguments are equal. Parameters  $\theta^*$  makes these equal by construction, therefore parameters  $\theta^*$  minimize the loss.  $\square$

This derivation shows that minimizing the SINCERE loss is a well-justified way to fit a tractable model for both the supervised contrastive classification task and the self-supervised instance discrimination task.

### 3.2. SINCERE Loss in Practice

The above analysis assumes a single target distribution of interest. In practice, a supervised classification problem with  $K$  classes requires learning  $K$  target-noise separation tasks. Following Khosla et al. (2020), we assume one shared function  $f_\theta$  approximates all  $K$  target-noise tasks for simplicity.

To approximate the expectation needed for the SINCERE loss in practice, we average over stochastically-sampled mini-batches  $(\mathcal{X}_b, \mathcal{Y}_b)$  of fixed size  $N$  from a much larger labeled dataset. These mini-batches are constructed from  $N/2$  images that then have 2 randomly sampled data augmentations applied to them. This incorporates terms similar to the self-supervised instance discrimination objective (Chen et al., 2020a) into SINCERE, as there will be  $N$  terms where 2 augmentations of the same image form the target distribution samples.

For each batch, we allow each index a turn as the selected target index  $S$ . For that turn, we define the target distribution as examples with class  $y_S$  and noise distributions as examples from other classes.

We thus fit neural net weights  $\theta$  by minimizing this expected loss over batches:

$$L(\theta) = \mathbb{E}_{\mathcal{X}_b, \mathcal{Y}_b} \left[ \sum_{S=1}^N \sum_{p \in \mathcal{P}} \frac{1}{N|\mathcal{P}|} L_{\text{SINCERE}}(z_S, z_p) \right], \quad (16)$$

$$L_{\text{SINCERE}}(z_S, z_p) = -\log \frac{e^{z_S \cdot z_p / \tau}}{e^{z_S \cdot z_p / \tau} + \sum_{n \in \mathcal{N}} e^{z_n \cdot z_p / \tau}}.$$

Our implementation of SINCERE uses the cosine similarity proposed by Wu et al. (2018) and averages over all same-class partners in  $\mathcal{P}$ . Other choices of similarity functions or pooling could be considered in future work.

Averaging over the elements of  $\mathcal{P}$  nonparametrically represents the target class  $y_S$  and encourages each  $z_p$  to have an embedding similar to its same-class partner  $z_S$ . However, no member of  $\mathcal{P}$  ever appears in the denominator without also appearing in the numerator. This avoids any repulsion between two members of the same class in the embedding space seen with SupCon loss. Intuitively, our SINCERE loss restores NCE’s assumption that the input used in the numerator belongs to the target distribution while all other inputs in the denominator belong to the noise distribution.

We note that SINCERE and SupCon have the same complexity in both speed and memory, as detailed in App. E.

### 3.3. Analysis of Gradients

We study the gradients of both SINCERE and SupCon to gain additional understanding of their relative properties.

The gradient of the SINCERE loss with respect to  $z_p$  is

$$\frac{z_S}{\tau} \left( \frac{e^{z_S \cdot z_p / \tau}}{\sum_{j \in \mathcal{N} \cup \{S\}} e^{z_j \cdot z_p / \tau}} - 1 \right) + \frac{\sum_{n \in \mathcal{N}} \frac{z_n}{\tau} e^{z_n \cdot z_p / \tau}}{\sum_{j \in \mathcal{N} \cup \{S\}} e^{z_j \cdot z_p / \tau}}. \quad (17)$$

The first term has a *negative* scalar times  $z_S$ . The second term has a *positive* scalar times each noise embedding  $z_n$ . Thus each gradient descent update to  $z_p$  encourages it to move *towards* the other target embedding  $z_S$  and *away* from each noise embedding  $z_n$ . The magnitude of these movements is determined by the softmax of cosine similarities. For a complete derivation and further analysis, see App. F.

This behavior is different from the gradient dynamics of SupCon loss. Khosla et al. (2020) provide SupCon’s gradient with respect to  $z_p$  as

$$\frac{z_S}{\tau} \left( \frac{e^{z_S \cdot z_p / \tau}}{\sum_{i \in \mathcal{I}} e^{z_i \cdot z_p / \tau}} - \frac{1}{|\mathcal{P}|} \right) + \frac{\sum_{n \in \mathcal{N}} \frac{z_n}{\tau} e^{z_n \cdot z_p / \tau}}{\sum_{i \in \mathcal{I}} e^{z_i \cdot z_p / \tau}}. \quad (18)$$

The scalar multiplying  $z_S$  in (18) will be in the range  $[\frac{-1}{|\mathcal{P}|}, 1 - \frac{1}{|\mathcal{P}|}]$ . The possibility of positive values implies  $z_p$  could be *pushed away* from  $z_S$  when applying gradient descent. In contrast, the scalar multiplier for  $z_S$  will always be in  $[-1, 0]$  for SINCERE in (17), which effectively

performs hard positive mining (Schroff et al., 2015). For further analysis of SupCon’s gradient, see App. G.

### 3.4. A Lower Bound on Idealized SINCERE Loss

van den Oord et al. (2018) motivate the self-supervised InfoNCE loss via an information-theoretic bound. We revisit this analysis for the more general case of SINCERE loss under the idealized settings of Sec. 3.1, where there is one target-noise task of interest.

In general, by the definition of loss  $L$  in Eq. (15) as an expectation of a negative log PMF, we can guarantee that  $L(\theta) \geq 0$ . However, we can prove a potentially tighter lower bound that depends on two quantities that define the difficulty of the contrastive learning task: the number of noise examples  $|\mathcal{N}|$  and the symmetrized KL divergence between the two true data-generating distributions: the target distribution  $p^+$  and the noise distribution  $p^-$ .

**Theorem 3.10.** *For any parameter  $\theta$  of the tractable model, let  $L(\theta)$  denote the idealized SINCERE loss computed as in Eq. (15) by averaging over samples of  $\mathcal{X}, S, \mathcal{P}$  from the true model in Eq. (12). Then we have*

$$L(\theta) \geq \log |\mathcal{N}| - (KL(p^- || p^+) + KL(p^+ || p^-)) \quad (19)$$

where we recognize the sum of the two KL terms as the symmetrized KL between  $p^+$  and  $p^-$ , the true data-generating PDFs for individual images  $x_i \in \mathcal{X}$ .

*Proof:* See App. C.

We emphasize this is a proper bound, while previous bounds for InfoNCE loss by van den Oord et al. (2018) required approximations. App. C provides further interpretation.

If  $p^+$  and  $p^-$  are known, this bound can characterize the “hardness” of the contrastive learning problem at hand, indicating what loss values are achievable. If the right hand side of the bound evaluates to a negative number, invoke the simpler earlier bound  $L(\theta) \geq 0$  instead.

This bound can also be used when  $p^+$  and  $p^-$  are unknown. As a corollary, a concrete numerical value of  $\log |\mathcal{N}| - L(\theta)$  can be interpreted as a lower bound on the symmetrized KL between the unknown  $p^+$  and  $p^-$ . We find it remarkable that a loss computed only via inner products of embedding vectors can be used to bound the divergence between distributions over a much higher dimensional data space. However, we caution that evaluations of  $L$  will be inexact in practice due to approximations of ideal expectation.

### 3.5. Related Work on Supervised Contrastive

Several works have expanded on SupCon loss in order to apply it to new problems. Feng et al. (2022) limit the target and noise distributions to K-nearest neighbors to allow for multi-modal class distributions. Kang et al. (2021) explicitly

set the number of samples from the target distribution to handle imbalanced datasets. Li et al. (2022b) introduce a regularization to push target distributions to center on uniformly distributed points in the embedding space. Yang et al. (2022) and Li et al. (2022a) utilize pseudo-labeling to address semi-supervised learning and supervised learning with noisy labels respectively. SINCERE loss can easily replace the use of SupCon loss in these applications.

Terms similar to the SINCERE loss have previously been used as a part of more complex losses. Chen et al. (2022) utilizes a loss like our SINCERE loss as one term of an overall loss function meant to spread out embeddings that share a class. Detailed discussion or motivation for the changes made to SupCon loss is not provided. Barbano et al. (2023) proposed  $\epsilon$ -SupInfoNCE loss, which eliminated the problematic denominator terms from SupCon for being “non-contrastive” and introduced a margin hyperparameter  $\epsilon$ . However, the paper focuses on using  $\epsilon$ -SupInfoNCE loss with an additional regularization for debiasing, so experiments do not investigate differences between  $\epsilon$ -SupInfoNCE loss and SupCon loss beyond classification accuracy.

## 4. Experiments

We evaluate SINCERE and SupCon losses for supervised classification on CIFAR-10, CIFAR-100 (Krizhevsky, 2009), and ImageNet-100 (Tian et al., 2020; Chun-Hsiao Yeh, 2022). A subset of CIFAR-10 containing only cat and dog images, referred to as CIFAR-2 here, was selected to evaluate binary classification. SupCon loss’ problematic behavior should be most pronounced on CIFAR-2 due to the large number of images sharing the same class.

Sec. 4.1 examines the differing behavior of SINCERE and SupCon losses during training. Sec. 4.2 shows how SINCERE better separates the target and noise distributions in the learned embedding space. Sec. 4.3 evaluates the accuracy of a k-nearest neighbor classifier on the learned embedding spaces. Sec. 4.4 evaluates transfer learning with a linear classifier. App. H provides details of the training process to aid in reproducing results with our shared code.

### 4.1. Training Loss

Table 1 reports loss values from training. SupCon and SINCERE losses return very similar values during the first training epoch but differ significantly by the final training epoch.

The analysis of SupCon loss in App. D suggests that including some target images as part of the noise distribution causes a decrease in the minimum loss value as the number of classes increases but batch size remains fixed. This occurs because the number of incorrectly labeled terms decreases as fewer inputs share a class in each batch. Table 1 clearly shows this in practice, with the final training loss value near

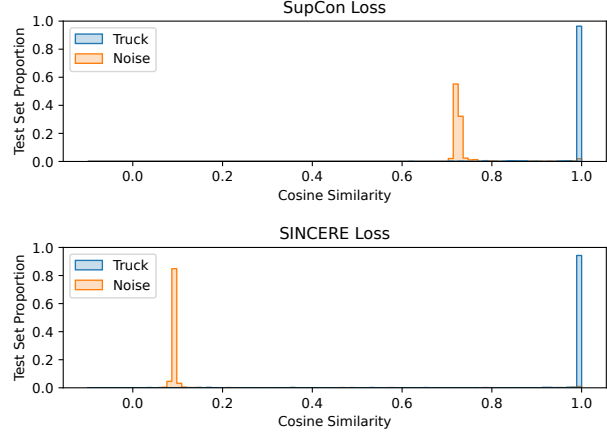


Figure 2. Histograms of cosine similarity values for CIFAR-10 test set nearest neighbors, comparing SupCon (top) and SINCERE (bottom). For each test image of the class “Truck,” its similarity to the nearest target image in the training set as well as the nearest noise image in the training set is plotted. SINCERE loss maintains high similarity for the target distribution while lowering the cosine similarity of the noise distribution more than SupCon loss.

the initial training loss value for CIFAR-2 and lowering as the number of classes increases.

Removing the incorrectly labeled terms results in SINCERE loss finishing training with lower loss values for all datasets. SupCon loss’ final training value remains higher than SINCERE loss even for the 100 class datasets where there are few incorrectly labeled terms.

### 4.2. Learned Embedding Space

Figure 2 visualizes the cosine similarity when the CIFAR-10 truck class is the target distribution and the noise distribution is formed by the other 9 classes. The truck class was chosen as a representative sample as the other classes follow the same trends seen here. All cosine similarities involve a member of the truck class from the test set and a member of the training set, visualizing the 1-nearest neighbor classification methodology from Sec. 4.3. The nearest neighbor from the train set target and train set noise distributions are plotted as “Truck” and “Noise” respectively. Both SINCERE loss and SupCon loss succeed at maximizing the similarity of the target distribution, but SINCERE loss lowers the similarity of heldout truck images to the noise distribution.

Table 2 quantifies this increase in separation by measuring the margin between the median similarity values of the target and noise distribution. SINCERE loss leads to larger margin (more target-noise separation) for all datasets. This confirms the picture in Fig. 1 and the analysis of SupCon loss’ gradient in Sec. 3.3: including the some target images as part of the noise distribution reduces the separation of target and noise distributions in the embedding space.

Training Loss	CIFAR-2		CIFAR-10		CIFAR-100		ImageNet-100	
	Initial	Final	Initial	Final	Initial	Final	Initial	Final
SupCon	6.94	6.28	6.94	4.69	6.91	2.37	6.92	2.35
SINCERE	6.25	<b>0.99</b>	6.80	<b>0.29</b>	6.91	<b>0.10</b>	6.91	<b>0.11</b>

Table 1. Average training loss values for initial and final training epochs. The final SINCERE loss value consistently approaches 0 regardless of the number of classes in the dataset. SupCon loss’ minimum decreases with more classes, which is seen in practice in the large variation in final loss value.

Training Loss	CIFAR-2	CIFAR-10	CIFAR-100	ImageNet-100
SupCon	0.410 (0.410, 0.411)	0.270 (0.269, 0.270)	0.438 (0.424, 0.448)	0.026 (0.025, 0.027)
SINCERE	<b>0.972 (0.972, 0.972)</b>	<b>0.854 (0.852, 0.855)</b>	<b>0.454 (0.444, 0.464)</b>	<b>0.154 (0.148, 0.159)</b>

Table 2. Margin between cosine similarity values for the test set target and noise distributions. The margin is calculated as the difference between each distribution’s median cosine similarity, analogous to the separation of distributions seen in Figure 2. 95% confidence interval values are reported in parentheses. SINCERE increases the size of the margin on all datasets.

### 4.3. Classification Accuracy

We measure classification accuracy for each trained embedding model via a weighted k-nearest neighbor evaluation on the test set. As in Wu et al. (2018), cosine similarity is used to choose the nearest neighbors and to weight votes. Previously, SupCon (Khosla et al., 2020) fit a linear classifier on frozen embeddings instead. However, those results show both methods have similar accuracy on CIFAR-10 and CIFAR-100 ( $\pm 0.5$  and  $\pm 0.04$  percentage points respectively). Therefore k-nearest neighbor was chosen to evaluate directly and simply on the learned embeddings.

Table 3 reports accuracy using 1 and 5-nearest neighbors. The difference between accuracies for SINCERE and SupCon is not statistically significant in all cases, based on the 95% confidence interval of the accuracy difference (Foody, 2009) from 1,000 iterations of test set bootstrapping.

These results are surprising given how different the learned embedding spaces of the methods are. We hypothesize that this occurs because SupCon loss is still a valid nonparametric classifier. The model learns an effective classification function, but does not optimize for further separation of target and noise distributions like InfoNCE and SINCERE.

### 4.4. Transfer Learning

Table 4 reports the accuracy for linear classifiers trained with frozen embeddings from SINCERE and SupCon models, which were trained on ImageNet-100. SINCERE improves accuracy for both Cars (Krause et al., 2013) and FGVC-Aircraft (Maji et al., 2013).

## 5. Discussion

The proposed SINCERE loss is a theoretically motivated loss for supervised noise contrastive estimation. Compared to the previous SupCon loss for the same task, SINCERE eliminates problematic repulsion of examples that share a class label while delivering competitive downstream accuracy and much better noise-target separation. For practitioners, SINCERE loss can be a “drop-in” replacement for SupCon loss, though we do suggest carefully refitting loss-weight hyperparameters for multi-term losses due to SINCERE’s broader range of values.

Future work may explore an alternative supervised loss which predicts all entries of the target distribution at once instead of individually. A naive approach to this problem would involve an exponential increase in the number of terms in the denominator, but could potentially model higher-order interactions between sets of samples instead of averaging over pair-wise interactions as is done currently.



Training Loss	CIFAR-2		CIFAR-10		CIFAR-100		ImageNet-100	
	1NN	5NN	1NN	5NN	1NN	5NN	1NN	5NN
SupCon	92.15	92.15	95.53	95.57	76.54	76.31	71.32	72.16
SINCERE	92.75	92.55	95.88	95.91	76.23	76.13	71.18	71.36

Table 3. Accuracy of k-nearest neighbor classifiers on test set. SINCERE’s performance is essentially indistinguishable from SupCon. No results are boldfaced, as differences are *not* statistically significant according to bootstrap interval analysis.

Training Loss	Aircraft (100)	Cars (196)
SupCon	38.6	46.1
SINCERE	<b>44.9</b>	<b>53.0</b>

Table 4. Top-1 accuracy for transfer learning from ImageNet-100. Number of classes in each dataset listed in parentheses.

## 6. Impact Statement

This paper presents work whose goal is to advance supervised feature learning and classification. There are many potential societal consequences of our work, with current methods impacting hiring (Drage & Mackereth, 2022), migration (Drage & Frabetti, 2023), the production of social norms and biases (Kupriianova & Kupriianova, 2023; Buolamwini & Gebru, 2018; Mehrabi et al., 2021; Leavy, 2018; West et al., 2019), and much more. We encourage responsible use of machine learning through methods such as those proposed by Mitchell et al. (2019), Gebru et al. (2021), and Prabhakaran et al. (2022).

## References

- Barbano, C. A., Dufumier, B., Tartaglione, E., Grangetto, M., and Gori, P. Unbiased supervised contrastive learning. In *The Eleventh International Conference on Learning Representations*, 2023. URL <https://openreview.net/forum?id=Ph5cJSfD2XN>.
- Buolamwini, J. and Gebru, T. Gender shades: Intersectional accuracy disparities in commercial gender classification. In *Conference on fairness, accountability and transparency*, pp. 77–91. PMLR, 2018.
- Caron, M., Misra, I., Mairal, J., Goyal, P., Bojanowski, P., and Joulin, A. Unsupervised Learning of Visual Features by Contrasting Cluster Assignments. In *Advances in Neural Information Processing Systems*, volume 33, pp. 9912–9924. Curran Associates, Inc., 2020. URL <https://proceedings.neurips.cc/paper/2020/hash/70feb62b69f16e0238f741fab228fec2-Abstract.html>.
- Chen, M., Fu, D. Y., Narayan, A., Zhang, M., Song, Z., Fatahalian, K., and Re, C. Perfectly balanced: Improving transfer and robustness of supervised contrastive learning. In Chaudhuri, K., Jegelka, S., Song, L., Szepesvari, C., Niu, G., and Sabato, S. (eds.), *Proceedings of the 39th International Conference on Machine Learning*, volume 162 of *Proceedings of Machine Learning Research*, pp. 3090–3122. PMLR, 17–23 Jul 2022. URL <https://proceedings.mlr.press/v162/chen22d.html>.
- Chen, T., Kornblith, S., Norouzi, M., and Hinton, G. A simple framework for contrastive learning of visual representations. In III, H. D. and Singh, A. (eds.), *Proceedings of the 37th International Conference on Machine Learning*, volume 119 of *Proceedings of Machine Learning Research*, pp. 1597–1607. PMLR, 13–18 Jul 2020a. URL <https://proceedings.mlr.press/v119/chen20j.html>.
- Chen, T., Kornblith, S., Swersky, K., Norouzi, M., and Hinton, G. E. Big Self-Supervised Models are Strong Semi-Supervised Learners. In *Advances in Neural Information Processing Systems*, volume 33, pp. 22243–22255. Curran Associates, Inc., 2020b. URL <https://proceedings.neurips.cc/paper/2020/hash/fcbc95ccdd551da181207c0c1400c655-Abstract.html>.
- Chen, X., Xie, S., and He, K. An empirical study of training self-supervised vision transformers. In *Proceedings of the IEEE/CVF International Conference on Computer Vision (ICCV)*, pp. 9640–9649, October 2021.
- Chun-Hsiao Yeh, Y. C. IN100pytorch: Pytorch implementation: Training resnets on imagenet-100. <https://github.com/danielchye/IN100pytorch>, 2022.
- Deng, J., Dong, W., Socher, R., Li, L.-J., Li, K., and Fei-Fei, L. Imagenet: A large-scale hierarchical image database. In *2009 IEEE Conference on Computer Vision and Pattern Recognition*, pp. 248–255, 2009. doi: 10.1109/CVPR.2009.5206848.
- Drage, E. and Frabetti, F. Copies without an original: the performativity of biometric bordering technologies. *Communication and Critical/Cultural Studies*, 0(0):1–19, 2023. doi: 10.1080/14791420.2023.

2292493. URL <https://doi.org/10.1080/14791420.2023.2292493>.
- Drage, E. and Mackereth, K. Does ai debias recruitment? race, gender, and ai’s “eradication of difference”. *Philosophy & technology*, 35(4):89, 2022.
- Fan, Z. MLE under model misspecification. Technical report, Stanford University, 2016. URL <https://web.stanford.edu/class/archive/stats/stats200/stats200.1172/Lecture16.pdf>.
- Feng, Y., Jiang, J., Tang, M., Jin, R., and Gao, Y. Re-thinking supervised pre-training for better downstream transferring. In *International Conference on Learning Representations*, 2022. URL <https://openreview.net/forum?id=Jjcv9MTqhcq>.
- Foody, G. M. Classification accuracy comparison: Hypothesis tests and the use of confidence intervals in evaluations of difference, equivalence and non-inferiority. *Remote Sensing of Environment*, 113(8):1658–1663, 2009. ISSN 0034-4257. doi: <https://doi.org/10.1016/j.rse.2009.03.014>. URL <https://www.sciencedirect.com/science/article/pii/S0034425709000923>.
- Geburu, T., Morgenstern, J., Vecchione, B., Vaughan, J. W., Wallach, H., Iii, H. D., and Crawford, K. Datasheets for datasets. *Communications of the ACM*, 64(12):86–92, 2021.
- Graf, F., Hofer, C., Niethammer, M., and Kwitt, R. Dissecting supervised contrastive learning. In Meila, M. and Zhang, T. (eds.), *Proceedings of the 38th International Conference on Machine Learning*, volume 139 of *Proceedings of Machine Learning Research*, pp. 3821–3830. PMLR, 18–24 Jul 2021. URL <https://proceedings.mlr.press/v139/graf21a.html>.
- Grill, J.-B., Strub, F., Altché, F., Tallec, C., Richemond, P., Buchatskaya, E., Doersch, C., Avila Pires, B., Guo, Z., Gheshlaghi Azar, M., Piot, B., kavukcuoglu, k., Munos, R., and Valko, M. Bootstrap Your Own Latent - A New Approach to Self-Supervised Learning. In *Advances in Neural Information Processing Systems*, volume 33, pp. 21271–21284. Curran Associates, Inc., 2020. URL <https://proceedings.neurips.cc/paper/2020/hash/f3ada80d5c4ee70142b17b8192b2958e-Abstract.html>.
- Gutmann, M. and Hyvärinen, A. Noise-contrastive estimation: A new estimation principle for unnormalized statistical models. In Teh, Y. W. and Titterton, M. (eds.), *Proceedings of the Thirteenth International Conference on Artificial Intelligence and Statistics*, volume 9 of *Proceedings of Machine Learning Research*, pp. 297–304, Chia Laguna Resort, Sardinia, Italy, 13–15 May 2010. PMLR. URL <https://proceedings.mlr.press/v9/gutmann10a.html>.
- Jaiswal, A., Babu, A. R., Zadeh, M. Z., Banerjee, D., and Makedon, F. A survey on contrastive self-supervised learning. *Technologies*, 9(1), 2021. ISSN 2227-7080. doi: 10.3390/technologies9010002. URL <https://www.mdpi.com/2227-7080/9/1/2>.
- Jing, L. and Tian, Y. Self-supervised visual feature learning with deep neural networks: A survey. *IEEE transactions on pattern analysis and machine intelligence*, 43(11): 4037–4058, 2020.
- Kang, B., Li, Y., Xie, S., Yuan, Z., and Feng, J. Exploring balanced feature spaces for representation learning. In *International Conference on Learning Representations*, 2021. URL <https://openreview.net/forum?id=OqtLIabPTit>.
- Khosla, P., Teterwak, P., Wang, C., Sarna, A., Tian, Y., Isola, P., Maschinot, A., Liu, C., and Krishnan, D. Supervised contrastive learning. In Larochelle, H., Ranzato, M., Hadsell, R., Balcan, M., and Lin, H. (eds.), *Advances in Neural Information Processing Systems*, volume 33, pp. 18661–18673. Curran Associates, Inc., 2020. URL [https://proceedings.neurips.cc/paper\\_files/paper/2020/file/d89a66c7c80a29b1bdbab0f2a1a94af8-Paper.pdf](https://proceedings.neurips.cc/paper_files/paper/2020/file/d89a66c7c80a29b1bdbab0f2a1a94af8-Paper.pdf).
- Krause, J., Stark, M., Deng, J., and Fei-Fei, L. 3d object representations for fine-grained categorization. In *Proceedings of the IEEE international conference on computer vision workshops*, pp. 554–561, 2013.
- Krizhevsky, A. Learning multiple layers of features from tiny images. 2009.
- Kupriianova, L. and Kupriianova, D. The ai in the porn industry of social media: Human replacement or precursor for growing the sexual violence and human trafficking indicators? *Collection of scientific papers "SCIENTIA"*, (October 6, 2023; Valencia, Spain):75–82, 2023.
- Le-Khac, P. H., Healy, G., and Smeaton, A. F. Contrastive representation learning: A framework and review. *IEEE Access*, 8:193907–193934, 2020. doi: 10.1109/ACCESS.2020.3031549.
- Leavy, S. Gender bias in artificial intelligence: The need for diversity and gender theory in machine learning. In *Proceedings of the 1st international workshop on gender equality in software engineering*, pp. 14–16, 2018.

- Li, S., Xia, X., Ge, S., and Liu, T. Selective-supervised contrastive learning with noisy labels. In *Proceedings of the IEEE/CVF Conference on Computer Vision and Pattern Recognition (CVPR)*, pp. 316–325, June 2022a.
- Li, T., Cao, P., Yuan, Y., Fan, L., Yang, Y., Feris, R. S., Indyk, P., and Katabi, D. Targeted supervised contrastive learning for long-tailed recognition. In *Proceedings of the IEEE/CVF Conference on Computer Vision and Pattern Recognition (CVPR)*, pp. 6918–6928, June 2022b.
- Lu, Z., Pu, H., Wang, F., Hu, Z., and Wang, L. The expressive power of neural networks: A view from the width. In *Advances in Neural Information Processing Systems (NeurIPS)*, 2017.
- Maji, S., Kannala, J., Rahtu, E., Blaschko, M., and Vedaldi, A. Fine-grained visual classification of aircraft. Technical report, 2013.
- Mehrabi, N., Morstatter, F., Saxena, N., Lerman, K., and Galstyan, A. A survey on bias and fairness in machine learning. *ACM computing surveys (CSUR)*, 54(6):1–35, 2021.
- Mitchell, M., Wu, S., Zaldivar, A., Barnes, P., Vasserman, L., Hutchinson, B., Spitzer, E., Raji, I. D., and Gebru, T. Model cards for model reporting. In *Proceedings of the conference on fairness, accountability, and transparency*, pp. 220–229, 2019.
- Murthy, K. R. Lower bound on  $\log \left( \sum_{i=1}^t x_i \right)$ . Mathematics Stack Exchange. URL <https://math.stackexchange.com/q/4068071>.
- Prabhakaran, V., Mitchell, M., Gebru, T., and Gabriel, I. A human rights-based approach to responsible ai. *arXiv preprint arXiv:2210.02667*, 2022.
- Schroff, F., Kalenichenko, D., and Philbin, J. Facenet: A unified embedding for face recognition and clustering. In *Proceedings of the IEEE Conference on Computer Vision and Pattern Recognition (CVPR)*, June 2015.
- Tian, Y., Krishnan, D., and Isola, P. Contrastive multiview coding. In *Computer Vision—ECCV 2020: 16th European Conference, Glasgow, UK, August 23–28, 2020, Proceedings, Part XI 16*, pp. 776–794. Springer, 2020.
- van den Oord, A., Li, Y., and Vinyals, O. Representation learning with contrastive predictive coding. *arXiv preprint arXiv:1807.03748*, 2018.
- Vaze, S., Han, K., Vedaldi, A., and Zisserman, A. Generalized category discovery. In *Proceedings of the IEEE/CVF Conference on Computer Vision and Pattern Recognition (CVPR)*, pp. 7492–7501, June 2022.
- West, M., Kraut, R., and Chew, H. E. Closing gender divides in digital skills through education. 2019. URL <https://en.unesco.org/EQUALS/voice-assistants>.
- White, H. Maximum likelihood estimation of misspecified models. *Econometrica: Journal of the econometric society*, 1982.
- Wu, Z., Xiong, Y., Yu, S. X., and Lin, D. Unsupervised feature learning via non-parametric instance discrimination. In *Proceedings of the IEEE Conference on Computer Vision and Pattern Recognition (CVPR)*, June 2018.
- Xu, B., Shen, F., and Zhao, J. Contrastive Open Set Recognition. *Proceedings of the AAAI Conference on Artificial Intelligence*, 37(9):10546–10556, June 2023. ISSN 2374-3468. doi: 10.1609/aaai.v37i9.26253. URL <https://ojs.aaai.org/index.php/AAAI/article/view/26253>. Number: 9.
- Yang, F., Wu, K., Zhang, S., Jiang, G., Liu, Y., Zheng, F., Zhang, W., Wang, C., and Zeng, L. Class-aware contrastive semi-supervised learning. In *Proceedings of the IEEE/CVF Conference on Computer Vision and Pattern Recognition (CVPR)*, pp. 14421–14430, June 2022.

Notation	Definition
$N$	number of elements in the dataset
$K$	number of labels such that $2 \leq K \leq N$
$(\mathcal{X}, \mathcal{Y})$	observed dataset with $N$ elements
$\mathcal{X} = (x_1, x_2, \dots, x_N)$	data (e.g. images)
$\mathcal{Y} = (y_1, y_2, \dots, y_N)$	categorical labels in $\llbracket 1, K \rrbracket$
$\mathcal{I} = \llbracket 1, N \rrbracket$	set of indices for elements in the dataset
$D$	dimensionality of neural network embeddings
$z_i \in \mathbb{R}^D$	neural network unit vector embedding of $x_i$
$\mathcal{T}$	indices for target distribution samples
$\mathcal{N} = \mathcal{I} \setminus \mathcal{T}$	indices for noise distribution samples
$T$	defines the number of samples from the target distribution; $2 \leq T \leq N - 1$
$\mathcal{P} \in \{I \subset \mathcal{I} \mid  I  = T - 1\}$	random variable for the set of indices for same-class partners for $t$
$S \in \mathcal{I} \setminus \mathcal{P}$	random variable defining the index of the target sample of interest
$f(x_i, y_j)$	score function outputting a scalar score representing how well data $x_i$ matches class representation $y_j$
$\tau$	temperature hyperparameter, typically about 0.1 in practice
$i \in \mathcal{I}$	index for arbitrary element of the dataset
$p \in \mathcal{P}$	index from the partners for $t$
$n \in \mathcal{N}$	index from the noise distribution
$j$	index used for clarity when another index notation already used, such as nested summations
$p^+(x_i)$	target data likelihood
$p^-(x_i)$	noise data likelihood
$p(\mathcal{X} S)$	data generating model for the self-supervised case
$p(S \mathcal{X})$	likelihood index $S$ is the index of the target class sample for the self-supervised case
$p(\mathcal{X} \mathcal{P}, S)$	data generating model for the self-supervised case
$p(S \mathcal{X}, \mathcal{P})$	likelihood $S$ is the index of the last target class sample for the supervised case
$\theta$	parameters of neural network $f_\theta$
$f_\theta(x_i, y_S)$	neural network used in the tractable model of the index likelihoods

Table A.1. Notation reference with abridged definitions.

## A. Notation Reference

See Table A.1.

## B. Proofs of Proposition 3.6

Given the assumed model in Eq. (12), we wish to show that the probability that a specific index  $S$  is the last remaining index of the target class is

$$p(S|\mathcal{X}, \mathcal{P}) = \frac{\frac{p^+(x_S)}{p^-(x_S)}}{\frac{p^+(x_S)}{p^-(x_S)} + \sum_{n \in \mathcal{N}} \frac{p^+(x_n)}{p^-(x_n)}} \quad (20)$$

where the set of “negative” indices is defined as  $\mathcal{N} = \{1, 2, \dots, N\} \setminus (\mathcal{P} \cup \{S\})$ . We emphasize that  $\mathcal{N}$  is determined by  $\mathcal{P}$ , the set of positive indices (other examples of the target class).

**Proof.** We can define the joint over  $S$  and  $\mathcal{P}$  given dataset  $\mathcal{X}$  via Bayes’ rule manipulations

$$p(S, \mathcal{P}|\mathcal{X}) = \frac{p(\mathcal{X}, S, \mathcal{P})}{p(\mathcal{X})} = \frac{p(\mathcal{X}|S, \mathcal{P})p(S, \mathcal{P})}{p(\mathcal{X})} \quad (21)$$

Plugging in basic model definitions from Eq. (12) into the numerator, and using shorthand  $u > 0$  to represent the uniform probability mass produced by evaluating  $p(S, \mathcal{P})$  at any valid inputs, we have

$$p(S, \mathcal{P}|\mathcal{X}) = \frac{\prod_{i \in \mathcal{P} \cup \{S\}} p^+(x_i) \prod_{n \in \mathcal{N}} p^-(x_n) \cdot u}{\sum_{\mathcal{R} \in \mathbb{P}_T} \left( \prod_{r \in \mathcal{R}} p^+(x_r) \prod_{m \in \mathcal{I} \setminus \mathcal{R}} p^-(x_m) \cdot u \right)} \quad (22)$$

where  $\mathbb{P}_T$  denotes the set of all possible subsets of indices  $\mathcal{I}$  with size exactly equal to  $T$ .



Next, apply two algebraic simplifications. First, cancel the  $u$  terms from both numerator and denominator. Second, multiply both numerator and denominator by  $\prod_{a \in \mathcal{I}} \frac{1}{p^-(x_a)}$  (a legal move with net effect of multiply by 1). After grouping each product into terms with ratio of  $p^+/p^-$  (which remain) and terms with  $p^-/p^-$  (which cancel away), we have

$$p(S, \mathcal{P}|\mathcal{X}) = \frac{\prod_{i \in \mathcal{P} \cup \{S\}} \frac{p^+(x_i)}{p^-(x_i)}}{\underbrace{\sum_{\mathcal{R} \in \mathbb{P}_T} \left( \prod_{r \in \mathcal{R}} \frac{p^+(x_r)}{p^-(x_r)} \right)}_{\Omega}} = \frac{1}{\Omega} \prod_{i \in \mathcal{P} \cup \{S\}} \frac{p^+(x_i)}{p^-(x_i)} \quad (23)$$

For convenience later, we define the denominator of the right hand side as  $\Omega$ , which is a constant with respect to  $S$  and  $\mathcal{P}$ .

Now, we wish to pursue our goal conditional of interest:  $p(S|\mathcal{P}, \mathcal{X})$ . Using Bayes rule on the joint  $p(S, \mathcal{P}|\mathcal{X})$  above, we have

$$p(S|\mathcal{P}, \mathcal{X}) = \frac{p(S, \mathcal{P}|\mathcal{X})}{p(\mathcal{P}|\mathcal{X})} \quad (24)$$

$$= \frac{p(S, \mathcal{P}|\mathcal{X})}{\sum_{j \in \mathcal{I} \setminus \mathcal{P}} p(S = j, \mathcal{P}|\mathcal{X})} \quad (25)$$

$$= \frac{\frac{1}{\Omega} \prod_{i \in \mathcal{P} \cup \{S\}} \frac{p^+(x_i)}{p^-(x_i)}}{\frac{1}{\Omega} \sum_{j \in \mathcal{I} \setminus \mathcal{P}} \prod_{\ell \in \mathcal{P} \cup \{j\}} \frac{p^+(x_\ell)}{p^-(x_\ell)}} \quad (26)$$

Finally, canceling terms that appear in both numerator and denominator (the  $\Omega$  term as well as the product over  $\mathcal{P}$ ), this leaves

$$p(S|\mathcal{P}, \mathcal{X}) = \frac{\frac{p^+(x_S)}{p^-(x_S)}}{\sum_{j \in \mathcal{I} \setminus \mathcal{P}} \frac{p^+(x_j)}{p^-(x_j)}} = \frac{\frac{p^+(x_S)}{p^-(x_S)}}{\frac{p^+(x_S)}{p^-(x_S)} + \sum_{n \in \mathcal{N}} \frac{p^+(x_n)}{p^-(x_n)}} \quad (27)$$

Where the last statement follows because  $\mathcal{I} \setminus \mathcal{P} = S \cup \mathcal{N}$  by definition of  $\mathcal{N}$ . We have thus reached the desired statement of equality.  $\square$ .

### C. Proofs of Bound relating SINCERE to Negative KL in Theorem 3.9

Assume the target class is known and fixed throughout this derivation. Further assume that both the target and noise distribution provide support over all possible data inputs  $x$ , so  $p^+(x) > 0$  and  $p^-(x) > 0$ .

We start with the definition of the loss as an expected negative log likelihood of the selected index  $S$  from Eq. (15).

$$L(\theta) = \mathbb{E}_{\mathcal{X}, S, \mathcal{P} \sim p_{true}} [-\log p_\theta(S|\mathcal{P}, \mathcal{X})] \quad (28)$$

where the expectation is with respect to samples  $\mathcal{X}, S, \mathcal{P}$  from the joint of the “true” model defined in Eq. (12).

Recall the optimal tractable model with weights  $\theta^*$  defined via target-to-noise density ratios in Prop. 3.8. The loss at this parameter is a lower bound of the loss at any parameter:  $L(\theta) \geq L(\theta^*)$ .

Now, substituting the definition of  $\theta^*$ , we find that by simplifying via algebra

$$\begin{aligned} L(\theta) \geq L(\theta^*) &= \mathbb{E}_{\mathcal{X}, S, \mathcal{P}} [-\log p_{\theta^*}(S|\mathcal{P}, \mathcal{X})] \\ &= \mathbb{E}_{\mathcal{X}, S, \mathcal{P}} \left[ -\log \frac{\frac{p^+(x_S)}{p^-(x_S)}}{\frac{p^+(x_S)}{p^-(x_S)} + \sum_{n \in \mathcal{N}} \frac{p^+(x_n)}{p^-(x_n)}} \right] \\ &= \mathbb{E}_{\mathcal{X}, S, \mathcal{P}} \left[ -\log \frac{1}{1 + \frac{1}{\frac{p^+(x_S)}{p^-(x_S)}} \sum_{n \in \mathcal{N}} \frac{p^+(x_n)}{p^-(x_n)}} \right] \\ &= \mathbb{E}_{\mathcal{X}, S, \mathcal{P}} \left[ \log \left( 1 + \frac{p^-(x_S)}{p^+(x_S)} \sum_{n \in \mathcal{N}} \frac{p^+(x_n)}{p^-(x_n)} \right) \right] \end{aligned} \quad (29)$$

Next, we invoke another bound, using the fact that  $\log 1 + p \geq \log p$  for any  $p > 0$  ( $\log$  is a monotonic increasing function).

$$\begin{aligned} L(\theta^*) &\geq \mathbb{E}_{\mathcal{X}, S, \mathcal{P}} \left[ \log \left( \frac{p^-(x_S)}{p^+(x_S)} \sum_{n \in \mathcal{N}} \frac{p^+(x_n)}{p^-(x_n)} \right) \right] \\ &= \underbrace{\mathbb{E}_{\mathcal{X}, S, \mathcal{P}} \left[ \log \sum_{n \in \mathcal{N}} \frac{p^+(x_n)}{p^-(x_n)} \right]}_A + \underbrace{\mathbb{E}_{\mathcal{X}, S, \mathcal{P}} \left[ \log \frac{p^-(x_S)}{p^+(x_S)} \right]}_B \end{aligned} \quad (30)$$

We handle terms A then B separately below.

**Term A:** Term A can be attacked by a useful identity: for any non-empty set of values  $a_1, \dots, a_L$ , such that all are strictly positive ( $a_\ell > 0$ ), we can bound of log-of-sum as

$$\log \left( \sum_{\ell=1}^L a_\ell \right) \geq \log L + \frac{1}{L} \sum_{\ell=1}^L \log a_\ell \quad (31)$$

This identity is easily proven via Jensen's inequality (credit to user Kavi Rama Murthy's post on Mathematics Stack Exchange ([Murthy](#))).

Using the above identity, our Term A of interest becomes

$$\begin{aligned} \text{term A} &= \mathbb{E}_{\mathcal{X}, S, \mathcal{P}} \left[ \log \left( \sum_{n \in \mathcal{N}} \frac{p^+(x_n)}{p^-(x_n)} \right) \right] \\ &\geq \mathbb{E}_{S, \mathcal{P}} \mathbb{E}_{\mathcal{X} \sim p(\mathcal{X}|S, \mathcal{P})} \left[ \log |\mathcal{N}| + \frac{1}{|\mathcal{N}|} \sum_{n \in \mathcal{N}} \log \frac{p^+(x_n)}{p^-(x_n)} \right] \end{aligned} \quad (32)$$

Under our model assumptions, the size of  $\mathcal{N}$  is fixed to  $N - T$  under Assumption 3.4 and does not fluctuate with  $S$  or  $\mathcal{P}$ . Furthermore, recall that given any known value of the target index  $S$ , all data vectors corresponding to noise indices  $\mathcal{N}$  are generated as i.i.d. draws from the noise distribution:  $x_n \sim p^-(\cdot)$ . These two facts plus linearity of expectations let us simplify the above as

$$\text{term A} \geq \log |\mathcal{N}| + \frac{1}{|\mathcal{N}|} \mathbb{E}_{S, \mathcal{P}} \left( \sum_{n \in \mathcal{N}} \int_{x_n} p^-(x_n) \left[ \log \frac{p^+(x_n)}{p^-(x_n)} \right] dx_n \right) \quad (33)$$

Next, realize that the inner integral is constant with respect to the indices choices defined by random variables  $S, \mathcal{P}$ . Furthermore, the sum over  $n$  simply repeats the same expectation  $|\mathcal{N}|$  times (canceling out the  $\frac{1}{|\mathcal{N}|}$  term). This leaves a compact expression for a lower bound on term A:

$$\begin{aligned} \text{term A} &\geq \log |\mathcal{N}| + \int_x p^-(x) \left[ \log \frac{p^+(x)}{p^-(x)} \right] dx \\ &= \log |\mathcal{N}| - \text{KL}(p^-(x) || p^+(x)). \end{aligned} \quad (34)$$

This reveals an interpretation of term A as a negative KL divergence from noise to target, plus the log of the size of negative set (a problem-specific constant).

**Term B:** The right-hand term B only involves the feature vector  $x_S$  at the target index  $S$  and not any other terms in  $\mathcal{X}$ . Thus, we can simplify the expectation over  $p(\mathcal{X}|S, \mathcal{P})$  as follows

$$\begin{aligned} \text{term B} &= \mathbb{E}_{\mathcal{X}, S, \mathcal{P}} \left[ \log \frac{p^-(x_S)}{p^+(x_S)} \right] = \mathbb{E}_{S, \mathcal{P}} \left[ \int_{\mathcal{X}} \log \left( \frac{p^-(x_S)}{p^+(x_S)} \right) p^+(x_S) \prod_{p \in \mathcal{P}} p^+(x_p) \prod_{n \in \mathcal{N}} p^-(x_n) d\mathcal{X} \right] \\ &= \mathbb{E}_{S, \mathcal{P}} \left[ \int \log \left[ \frac{p^-(x_S)}{p^+(x_S)} \right] p^+(x_S) dx_S \right] \end{aligned} \quad (35)$$

where we got all other  $x_p$  and  $x_n$  terms to simplify away because integrals over their PDFs evaluate to 1.

Now, we can recognize what remains above as a negative KL divergence. Let's write this out explicitly, replacing  $x_S$  with notation  $x$  (no subscript) simply to reinforce that the KL term inside the expectation does not vary with  $S$  (regardless of

which index is chosen, the target and noise distributions compared by the KL will be the same). This yields

$$\text{term B} = \mathbb{E}_{S, \mathcal{P}} \left[ \int \log \left[ \frac{p^-(x)}{p^+(x)} \right] p^+(x) dx \right] \quad (36)$$

$$= -\mathbb{E}_{S, \mathcal{P}} [\text{KL}(p^+(x) || p^-(x))] \quad (37)$$

$$= -\text{KL}(p^+(x) || p^-(x)) \quad (38)$$

where in our ultimate expression, we know the KL is constant w.r.t.  $S, \mathcal{P}$ . Thus, the expectation simplifies away (writing out the full expectation as a sum then bringing the KL term outside leaves a PMF that sums to one over the sample space).

This reveals an interpretation of term B as a negative KL divergence from target to noise.

**Combining terms A and B.** Putting it all together, we find

$$L(\theta) \geq L(\theta^*) \geq \log |\mathcal{N}| - \underbrace{(\text{KL}(p^-(x) || p^+(x)) + \text{KL}(p^+(x) || p^-(x)))}_{\text{symmeterized KL divergence}} \quad (39)$$

Thus, every evaluation of our proposed SINCERE loss has an information-theoretic interpretation as an upper-bound on the sum of the log of the size of the noise samples and the negative *symmeterized* KL divergence between the target and noise distributions. For a definition of symmeterized KL divergence see [this link to Wikipedia](#)

**Interpretation.** The bound above helps quantify what loss values are possible, based on two problem-specific elementary facts: the symmeterized divergence between target and noise distributions (where larger values mean the target-noise distinction is easier) and the total number of noise samples.

Naturally, the more trivial lower bound for  $L(\theta)$  is zero, as that is the lowest any negative log PMF over any discrete variable (like  $S$ ) can go. We observe that our proposed bound can often provide more information than this trivial one, as large  $|\mathcal{N}|$  will push the bound well above zero.

We further observe the following:

- Larger symmeterized KL will lower the RHS of the bound, indicating loss values can go lower. This intuitively makes sense: when target and noise distributions are easier to separate, we can get closer and closer to “perfect” predictions of  $S$  with our tractable model and thus PMF values  $p_\theta(S | \mathcal{X}, \mathcal{P})$  approach 1 and  $L$  approaches 0.
- As the total number of noise samples gets higher, the RHS of the bound gets larger. This also makes sense, as the problem becomes harder (more chances to guess wrong when distinguishing between the one target sample and many noise samples), our expected loss should also increase.

**Relation to previous bounds derived for InfoNCE.** [van den Oord et al. \(2018\)](#) derive a bound relating their InfoNCE loss to a mutual information quantity in the self-supervised case. Indeed, our derivation of our bound was inspired by their work. Here, we highlight three key differences between our bound and theirs.

First, our bound applies to the more general supervised case, not just the self-supervised case.

Second, following their derivation carefully, notice that the claimed bound requires an *approximation* in their Eq. 8 in the appendix “A.1 Estimating the Mutual Information with InfoNCE” of [van den Oord et al. \(2018\)](#). While they argue this approximation becomes more accurate as batch size  $N$  increases, indeed for any finite  $N$  the claim of a strict bound is not guaranteed. In contrast, our entire derivation above requires no approximation.

Finally, the relation derived in [van den Oord et al. \(2018\)](#) is expressed in terms of mutual information, not symmeterized KL divergence. This is due to their choice to write the noise distribution as  $p(x_i)$  and the target distribution as  $p(x_i|c)$  where index  $c$  denotes the target class of interest. For us, these two choices imply the noise and target are related by the sum rule

$$p(x_i) = \sum_{c'} p(c') p(x_i | c') \quad (40)$$

over an extra random variable  $c$  whose sample space and PMF are not extremely clear, at least in our reading of [van den Oord et al. \(2018\)](#). In contrast, our formulation throughout Sec. 3.1 of the main paper fixes one target and one noise distribution throughout. We think this is a conceptually cleaner approach.

## D. Comparison to SupCon Probability

Attempting to translate SupCon loss into the noise-contrastive paradigm suggests that it assigns probability to the data point at index  $S$  out of all possible data points via

$$\frac{\frac{p^+(x_S)}{p^-(x_S)}}{\frac{p^+(x_S)}{p^-(x_S)} + \sum_{j \in \mathcal{P} \setminus \{p\}} \frac{p^+(x_j)}{p^-(x_j)} + \sum_{n \in \mathcal{N}} \frac{p^+(x_n)}{p^-(x_n)}}. \quad (41)$$

We emphasize that this does *not* correspond to a principled derivation from a coherent probabilistic model. In fact, it is not a softmax over values of  $S$  because the sum of these values over all valid  $S$  is less than 1. In contrast, our derivation of SINCERE follows directly from the model in (12). Furthermore, this framing of SupCon makes clear that the additional denominator terms penalize similarity between embeddings from the target distribution, which results in the problematic within-class repulsion behavior described in Fig. 1.

## E. Runtime and Memory Complexity

Given a batch of  $N$  data points, each with a  $D$ -dimensional embedding, SINCERE or SupCon loss can be computed in  $O(N^2 D)$  time, with quadratic complexity arising due to need for computation of dot products between many pairs of embeddings. An implementation that was memory sensitive could be done with  $O(ND)$  memory, which is the cost of storing all embedding vectors. Our implementation has memory cost of  $O(N^2 + ND)$ , as we find computing all  $N^2$  pairwise similarities at once has speed advantages due to vectorization. In our experiments with a batch size of 512, we find the runtime of computing embeddings with the forward pass of a neural network far exceeds the runtime of computing losses given embeddings.

## F. Further Analysis of Gradients

The gradient of the SINCERE loss with respect to  $z_t$  is  $\frac{\delta}{\delta z_t} L_{\text{SINCERE}}(z_t)$

$$= \frac{\delta}{\delta z_t} \frac{-1}{|\mathcal{P}_t|} \sum_{p \in \mathcal{P}_t} \log \frac{e^{z_t \cdot z_p / \tau}}{e^{z_t \cdot z_p / \tau} + \sum_{i \in \mathcal{N}_t} e^{z_t \cdot z_i / \tau}} \quad (42)$$

$$= \frac{\delta}{\delta z_t} \frac{-1}{|\mathcal{P}_t|} \sum_{p \in \mathcal{P}_t} \left( \frac{z_t \cdot z_p}{\tau} - \log \sum_{i \in \mathcal{N}_t \cup \{p\}} e^{z_t \cdot z_i / \tau} \right) \quad (43)$$

$$= \frac{-1}{\tau |\mathcal{P}_t|} \sum_{p \in \mathcal{P}_t} \left( z_p - \frac{\sum_{i \in \mathcal{N}_t \cup \{p\}} z_i e^{z_t \cdot z_i / \tau}}{\sum_{i \in \mathcal{N}_t \cup \{p\}} e^{z_t \cdot z_i / \tau}} \right) \quad (44)$$

$$= \frac{-1}{\tau |\mathcal{P}_t|} \sum_{p \in \mathcal{P}_t} \left( z_p - \frac{z_p e^{z_t \cdot z_p / \tau} + \sum_{i \in \mathcal{N}_t} z_i e^{z_t \cdot z_i / \tau}}{\sum_{i \in \mathcal{N}_t \cup \{p\}} e^{z_t \cdot z_i / \tau}} \right) \quad (45)$$

$$= \frac{1}{\tau |\mathcal{P}_t|} \sum_{p \in \mathcal{P}_t} \left( z_p \left( \frac{e^{z_t \cdot z_p / \tau}}{\sum_{i \in \mathcal{N}_t \cup \{p\}} e^{z_t \cdot z_i / \tau}} - 1 \right) + \frac{\sum_{i \in \mathcal{N}_t} z_i e^{z_t \cdot z_i / \tau}}{\sum_{i \in \mathcal{N}_t \cup \{p\}} e^{z_t \cdot z_i / \tau}} \right). \quad (46)$$

## G. Effect of SupCon Gradient

SupCon’s possible repulsion between members of the same class increases in severity as  $|\mathcal{P}|$  increases, resulting in a scalar in  $[0, 1]$  as  $|\mathcal{P}|$  approaches positive infinity. Khosla et al. (2020) previously hypothesized that the  $\frac{-1}{|\mathcal{P}|}$  term came from taking the mean of the embeddings  $z_p \in \mathcal{P}$ . Our analysis suggests it is actually due to improperly including target class examples other than  $S$  and  $p$  in the loss’ denominator.

A similar issue arises from the summation over the noise distribution in (18). Each softmax includes the noise distribution and the entire target distribution in the denominator instead of only the noise distribution and  $z_p$  as in (17). This reduces the SupCon loss’ penalty on poor separation between the noise and target distributions.



---

## H. Training and Hyperparameter Selection

Models were trained on a Red Hat Enterprise Linux 7.5 server with a A100 GPU with 40 GiB of memory and 16 Intel Xeon Gold 6226R CPUs. Many of the CPUs were primarily used for parallelization of data loading, so fewer or smaller CPUs could be used easily. PyTorch 2.0.1 and Torchvision 0.15.2 for CUDA 12.1 were used for model and loss implementations.

A hyperparameter search was done for each SupCon and SINCERE loss model with 10% of the training set used as validation. Training was done with 800 epochs of stochastic gradient descent with 0.9 momentum, 0.0001 weight decay, 512 batch size, and a cosine annealed learning rate schedule with warm-up, which spends 10 epochs warming up from 0.1% to 100% then cosine anneals back to 0.1% at the last epoch. Various settings of temperature ( $\tau$ ) and learning rate were evaluated, with the highest 1NN accuracy determining the final model parameters. The final models were trained on the entire training set, with evaluations on the test set reported in the main paper.

Transfer learning results used the SINCERE and SupCon ImageNet-100 models as frozen feature extractors for linear classifiers. This differs from the full model finetuning method used by [Khosla et al. \(2020\)](#) in order to more clearly determine the effects of the frozen embedding features. Our reported transfer learning accuracy results are more comparable to the transfer learning results by [Chen et al. \(2020a\)](#), although they opt for L-BFGS optimization without data augmentation instead of our choice of SGD optimization with random crops and horizontal flips. Training was done with 100 epochs of stochastic gradient descent with 0.9 momentum, 0.0001 weight decay, and 128 batch size. Various learning rates were evaluated, with the highest classification accuracy on the 10% of the training set used as validation determining the final model parameters. The final models were trained on the entire training set, with evaluations on the test set reported in the main paper.